CHAPTER 1

INTRODUCTION

1.1 Background of Study

Injection wells are found in many oil and gas fields located in the counties where oil and gas are produced. The water injection method used in oil production is where water is injected back into the reservoir to increase pressure and thereby stimulate production. Water injection wells can be found both onshore and offshore. This method is used to increase oil recovery from an existing reservoir. Water is injected for two main reasons which are for pressure support of the reservoir (also known as voidage replacement) and to sweep or displace the oil from the reservoir, and push it towards an oil production well. Normally only 30% of the oil in a reservoir can be extracted, but water injection increase that percentage (known as the recovery factor) and maintain the production rate of a reservoir over a longer period of time [1]. The water injection principle is water need to push the oil towards the wells like a piston. The result of the injection is not quick, it needs time.

After a well is drilled, often to depths over 5,000 feet, steel pipe called casing is cemented in the hole [2]. The casing and cement prevent fluids in different zones from mixing with each other or with injected fluids. The casing and cement are perforated opposite the injection zone. To provide an extra layer of protection, tubing is placed in the well to a point just above the perforations and a packer is used near the bottom of the tubing to seal it against the casing. The packer prevents water from entering the space between the tubing and casing when water is injected down the tubing. Several tests are run to make sure the well is operating properly and the injected fluids are

confined to the intended injection zone. An injection zone is usually sandstone, a rock porous and permeable enough to accept injected fluids.

Seawater is obviously the most convenient source for offshore production facilities [1]. Produced water is often used as an injection fluid. This reduces the potential of causing formation damage due to incompatible fluids, although the risk of scaling or corrosion in injection flowlines or tubing remains. Also, the produced water, being contaminated with hydrocarbons and solids, must be disposed of in some manner, and disposal to sea will require a certain level of clean-up of the water stream first. After oil and gas are separated from the produced water at the producing well, the water is piped or trucked to the injection site. There, the water is transferred to holding tanks and pumped down to the injection well.

1.2 Problem Statement

Most of Carbon Steel tubing for Water Injection wells at Dulang Fields was badly corroded even though wells were completed with the new downhole tubing. In order to avoid or minimize the tubing internal corrosion problems, the study on microstructure of the tubing parts should be done especially on how to improve the material of the tubing.

1.3 Objective and Scope of Study

The objective of the study is to determine the primary cause of a failure by investigating the corroded parts and to provide with the suggested improvement of suitable material for the downhole tubing. Also, to study on the microstructure of the Carbon Steel tubing i.e. whether the part has experience extreme heat, cold work, reveal crack and fatigue. The scope of the study covered on the analysis of material for Carbon Steel tubing by using optical microscope (OM) and scanning electron microscope (SEM) attached with

the energy dispersive x-ray spectroscopy (EDX/EDS). The determination of the failure was performed on well Dulang A-29L.

CHAPTER 2

LITERATURE REVIEW

2.1 Failure Analysis

Failure analysis is the process of collecting and analyzing data to determine the cause of a failure and how to prevent it from recurring. It is an important discipline in many branches of manufacturing industry, such as the electronics industry, where it is a vital tool used in the development of new products and for the improvement of existing products [3].

Failure analysis and prevention are important functions to all of the engineering disciplines. The materials engineer often plays a lead role in the analysis of failures, whether a component or product fails in service or if failure occurs in manufacturing or during production processing [3]. In any case, one must determine the cause of failure to prevent future occurrence and to improve the performance of the device, component or structure.

2.2 Carbon Steel

Carbon steel, also called plain carbon steel, is steel where the only main alloying constituent is carbon; the other elements present are in quantities too small to affect the properties. The only other elements allowed in carbon steel are manganese (1.65% max), silicon (0.60% max), and copper (0.60% max) [4]. Steel with low carbon content has properties similar to iron. As the carbon content rises, the metal becomes harder and stronger but less ductile and more difficult to weld. In general, higher carbon content

lowers the melting point and its temperature resistance [4]. Typical compositions of carbon:

- *Mild (low carbon) steel*: approximately 0.05–0.15% carbon content for low carbon steel and 0.16-0.29% carbon content for mild steel (e.g. AISI 1018 steel) [4]. Mild steel has a relatively low tensile strength, but it is cheap and malleable; surface hardness can be increased through carburizing.

- *Medium carbon steel*: approximately 0.30–0.59% carbon content (e.g. AISI 1040 steel) [4]. Balances ductility and strength and has good wear resistance; used for large parts, forging and automotive components.

- *High carbon steel*: approximately 0.6–0.99% carbon content [4]. Very strong, used for springs and high-strength wires.

- *Ultra-high carbon steel*: approximately 1.0–2.0% carbon content. Steel that can be tempered to great hardness [4]. Used for special purposes like (non-industrial-purpose) knives, axles or punches. Most steels with more than 1.2% carbon content are made using powder metallurgy and usually fall in the category of high alloy carbon steels [4].

2.3 Corrosion of Carbon Steel

Carbon steel, the most widely used engineering material, accounts for approximately 85%, of the annual steel production worldwide [5]. Despite its relatively limited corrosion resistance, carbon steel is used in large tonnages in marine applications, nuclear power and fossil fuel power plants, transportation, chemical processing, petroleum production and refining, pipelines, mining, construction and metal-processing equipment.

2.3.1 Classification of Corrosion

There are several types of corrosion that will be addressed such as:

- *Atmospheric corrosion*: the corrosion of carbon steel in the atmosphere is best understood from a film formation and brake down standpoint. It is an inescapable fact that iron in the presence of oxygen and water is thermodynamically unstable with respect to its oxides. Rusting of iron depends on relative humidity and time of exposure in atmosphere containing 0.01% SO_2 [5]. The increase in corrosion rate produced by the addition of SO_2 is substantial. Oxides of nitrogen in the atmosphere would also exhibit an accelerating effect on the corrosion of steel. Indeed, any gaseous atmospheric constituent capable of strong electrolytic activity should be suspected as being capable of increasing the corrosion rate of steel.

- *Soil Corrosion*: the response of carbon steel to soil corrosion depends primarily on the nature of the soil and certain other environmental factors, such as the availability to moisture and oxygen. These factors can lead to extreme variations in the rate of the attack. Soils with high moisture content, high electrical conductivity, high acidity, and high dissolved salts will be most corrosive [5]. The effect of aeration on soils is somewhat different from the effect of aeration in water because poorly aerated conditions in water can lead to accelerated attack by sulfate-reducing anaerobic bacteria.

- *Aqueous Corrosion*: Carbon steel pipes and vessels are often required to transport water or are submerged in water to some extent during service. This exposure can be under conditions varying temperature, flow rate, pH, and other factors, all of which can alter the rate of corrosion [5]. The relative acidity of the solution is probably the most important factor to be considered. At low pH the evolution of hydrogen tends to eliminate the possibility of protective film formation so that steel continues to corrode but in alkaline solutions, the formation of protective films greatly reduces the corrosion rate [5]. The greater alkalinity, the slower the rate of attack becomes. In neutral solutions, other factors such as aeration, became determining so that generalization becomes more difficult.

2.3.1.1 Aqueous Corrosion

1. *Seawater Corrosion*: over 70% of the surface of the earth is covered with seawater. This makes seawater the most widespread corrosive medium next to the atmosphere. Most metals, alloys and construction materials are corroded by seawater and marine atmosphere. The conditions of exposure are the main parameters determining the behaviour of different materials. The rate of corrosion in seawater is determined mainly by the amount of oxygen that reaches the cathode, whereby the electrolyte resistance is of no consequence due to the large cross-section and good conductivity [13]. Due to good conductivity of the medium, the anode and cathode of a corrosion cell in seawater can be some distance apart. The marine atmosphere is characterized by a raised content of salt particles carried on the wind from the sea spray. The salt content of seawater is defined as the total mass of salt in solution in 1 kg of seawater. Seawater in the open sea far from land in the major oceans has an average salt content within the range of 32-37.5 g/kg. This salt content shows considerable consistency in given regions and throughout the years. The salt content can be calculated based on the chloride ion content as per [13]:

Salt content in % = (1.81 x chloride ion content in %) + 0.003

The pH level of seawater is generally 7.7 – 8.2. As the chloride content increases, not only do the electrical conductivity of the electrolyte solution and thus the activity of the corroding elements increase. Usually the cause of failure in chloride containing solutions is pitting corrosion although this depends on the Cl^- ion concentration.

2.3.2 Forms of Corrosion

The forms of corrosion are classified in the following three categories [10]:

- *Uniform corrosion:* even and regular loss of metal from the corroding surface.
- *Localized corrosion:* all or most of the metal loss occurs at discrete areas.
- *Galvanic corrosion:* occasions by electrical contact between dissimilar conductors in an electrolyte.

2.3.2.1 Localized Corrosion

1. *Pitting Corrosion:* localized form of corrosion by which cavities or holes are produced in the material. Pitting is considered to be more dangerous than uniform corrosion damage because it is more difficult to detect, predict and design against. Corrosion products often cover the pits. A small, narrow pit with minimal overall metal loss can lead to the failure of an entire engineering system. Pitting corrosion is almost a common denominator of all types of localized corrosion attack but may assume different in shapes. Its can produce pits with their mouth open (uncovered) or covered with a semi-permeable membrane of corrosion products. Pits can be either hemispherical or cup-shaped. The following are some factors contributing to initiation and propagation of pitting corrosion:
    - Localized chemical or mechanical damage to a protective oxide film.
    - Water chemistry factors that can cause breakdown of a passive film such as acidity, low dissolved oxygen

concentrations which tend to render a protective oxide film less stable and high chloride concentration.

- Localized damage to a poor application of a protective coating.
- The presence of nonuniformities in the metal structure of the component, for example, nonmetallic inclusions.

a. *Pitting Mechanism:* It is supposed by some that gravitation causes downward-oriented concentration gradient of the dissolved ions in the hole caused by the corrosion, as the concentrated solution is denser. The acidity inside the pit is maintained by the spatial separation of the cathodic and anodic half-reactions, which creates a potential gradient and electromigration of aggressive anions into the pit [11].

   Thus, it will cause little loss of material with small effect on its surface, while it damages the deep structures of the metal. The pits on the surface are often obscured by corrosion products.

b. *Environmental Factors:* The presence of chlorides, for example, in sea water, significantly aggravates the conditions for formation and growth of the pits through an autocatalytic process. The pits become loaded with positive metal ions through anodic dissociation. The Cl- ions become concentrated in the pits for charge neutrality and encourage the reaction of positive metal ions with water to form a hydroxide corrosion product and H+ ions. Hence, the pits are weakly acidic, which accelerates the process. Besides chlorides, other anions implicated in pitting include thiosulfates ($S_2O_3^{2-}$), fluorides and iodides. Stagnant water conditions favour pitting. Thiosulfates are

particularly aggressive species and are formed by partial oxidation of pyrite, or partial reduction of sulphate [11]. Thiosulfates are a concern for corrosion in many industries like sulfide ores processing, oil wells and pipelines transporting soured oils, photographic industry, methionine and lysine factories. Corrosion inhibitors, when present in sufficient amount, will provide protection against pitting. However, too low level of them can aggravate pitting by forming local anodes.

2. *Crevice Corrosion:* occurs in cracks or crevices formed between mating surfaces of metal assemblies and usually take the form of pitting or etched patches. Both surfaces maybe of the same metal or dissimilar metal or one surface maybe a nonmetal. It can also occur under scale and surface deposits and under loose fitting of washers and gaskets that do not prevent the entry of liquid between them and the metal surface. Crevices may proceed inward from a surface exposed to the air or may exist in an immersed structure [12]. The aggravating factors present in a fully developed crevice can be summarized in the following points:

    - Metal ions produced by the anodic corrosion reaction readily hydrolyze giving off protons (acid) and forming corrosion products. The pH in a crevice can reach very acidic values.
    - The acidification of the local environment can produce a serious increase in the corrosion rate of most metals.
    - The corrosion products seal even further the crevice environment.
    - The accumulation of positive charge in the crevice becomes a strong attractor to negative ions in the environment such as

chlorides and sulphates that can be corrosive in their own right.

a. *Crevice Mechanism:* Crevices can develop a local chemistry which is very different from that of the bulk fluid.

   Two factors are important in the initiation of active crevice corrosion were the chemical composition of the electrolyte in the crevice and the potential drop into the crevice [12]. Both the potential drop and the change in composition of the crevice electrolyte are caused by deoxygenation of the crevice and a separation of electroactive areas, with net anodic reactions occurring within the crevice and net cathodic reactions occurring exterior to the crevice. The mechanism of crevice corrosion can be similar to that of pitting corrosion. However, there are sufficient differences to warrant a separate treatment.

b. Environmental Factors: the deposit attack may produce crevice corrosion. The deposit acts as a shield and creates a stagnant condition there under. The deposit could also be a permeable corrosion product. Contact between metal and non-metallic surfaces can cause crevice corrosion act as in the case of gasket. Crevice attack begins and progresses in the area where the metal and rubber are in contact. In order to function as a corrosion site, a crevice must be wide enough to permit liquid entry but sufficiently narrow to maintain a stagnant zone. For this reason, crevice corrosion usually occurs at openings a few thousands of an inch or less in width [12].

2.4 Steel Tubular Manufacturing Process

According to American Petroleum Institute standard for casing and tubing (API 5CT), the grade of L80 pipe furnished at the specified specification shall be made to a fine austenitic grain size. The pipe furnished shall be made by seamless (S) or electric weld (EW) process as per requested by the purchaser [14]. Seamless pipe is defined as a wrought steel tubular product made without a welded seam. It is manufactured by hot working steel or if necessary, by subsequently cold finishing the hot worked tubular product to produce the desired shape, dimensions and properties. Meanwhile, the electric welded pipe is defined as pipe having one longitudinal seam formed by electric resistance or electric induction welding without the addition of filler metal, wherein the edges to be welded are mechanically pressed together and the heat for welding is generated by the resistance to flow of electric current. The weld seam of electric welded pipe shall be heat treated after welding to a minimum temperature of 1000°F or 538°C or processed in such a manner that no untempered martensite remains.

2.4.1 Steel Tubular Heat Treatment

In accordance to API 5CT, the grade L80 pipe shall be heat treated by quenched and tempered in order to produce a desired microstructure or mechanical properties. The type of L80 pipe shall be full body heat treated and air quenched by attaining a minimum tempering temperature of 1050°F or 566°C.

2.4.2 Mechanical Properties of Steel Tube

The mechanical properties requirements for grade L80 pipe is specified in Table 2.1 [8,14].

Table 2.1: Mechanical Properties of Steel Tube.

Standard codes	Models of steel tubes	Tensile strength (psi/Mpa)	Yield strength (psi/Mpa)	Hardness requirement
API SPEC 5CT	L80 Type 1	95,000 (655)	80,000 (552)	21- 23 HRC

2.4.3 Chemical Composition of Steel Tube

The pipe furnished to this specification (see Table 2.1) shall be subjected the chemical requirements specified in Table 2.2 for the grade and type specified [8,14].

Table 2.2: Chemical Composition of Steel Tube.

Standard codes	Grade of steel tubular	Chemical compositions (%)						
		C	Mn	Ni	Cu	P	S	Si
API SPEC 5CT	L80 Type 1	≤ 0.43	≤ 1.90	≤ 0.25	≤ 0.35	≤ 0.03	≤ 0.03	≤ 0.45

2.5 Background History

Well Dulang A-29 (DLA-29) was completed in April 1994 as dual completion injector in the E-2, E-7, E-12/13 and E-14 reservoirs. DLA-29 is a directional well with maximum inclination of 65 degree, which was drilled in 1994 with total depth (TD) at 2670.59 m-MDDF or 1463.09 m-TVD [6]. The short string (DLA-29S) injector is accessible to E-2 and E-7 while long string (DLA-29L) injector is accessible to E-12/13 and E-14. The initial injection rate from long string well on 1996 was about 1500 BWPD before levelling at 3000 BWPD until end of year 2000 [6]. On the other hand, the initial injection rate from short string in 1998 was about 3000 BWPD until middle

2002 [6]. In 2004, Production Logging Tool (PLT) and Multi-finger Imaging Tool (MIT) surveys confirmed severe leaking in the long string of DLA-29 (refer to Appendix I) which was impacted in declining of the recovery due to loss of good pressure maintenance for E-7, E-12/13 and E-14 [7]. Thus, the long string was shut-in in 2004 after MIT confirmed over 30 leak points along the internal tubing wall (refer to Figure 2.1).

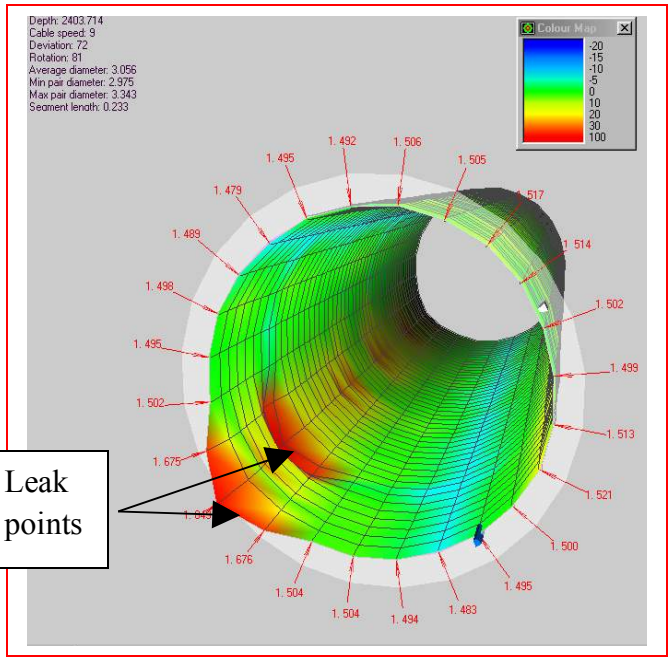

Figure 2.1: Multiple holes detected at 2403.71m MDBDF.

2.6 Similar Cases Happen

2.6.1 Case I

Well Dulang A-32 (DLA-32) was completed on 31 March 1994 as dual string which is Long String (LS) as water injector that injecting to E12/13 & E14 reservoir, meantime Short String (SS) as oil producer that producing from E7 reservoir. LS is injecting around 3,264 BWPD and SS is currently shut in since producing water [6]. Production logging recently has been run on LS in March 2007 and found severely many leaking point above upper packer and on blast joint in front of E7 sand (refer to Appendix II).

2.6.2 Case II

Well Dulang C-25 (DLC-25) is never been perforate since completed on March 1995 however this well was suspected suffered the 'Tubing leaks' problem above top packer due to PCP-THP communications [7]. A lot of time spends on this well in other to locate the leak points via conventional Tubing integrity test and 'Ponytail' run via slick line and fail to locate the exact leak points. In January 2004, MIT was run and locate the multiple holes at top section (Tubing joint #3) of the well (refer to Appendix III).

CHAPTER 3

METHODOLOGY

3.1 Procedure for Failure Analysis

The report was briefed on the description of how the failure analysis investigations have been going on and the methods used to prepare the samples for fractography and metallography. The investigations began where steel tubing cut sample was received for analysis. This was immersed into a chemical solution for a day in order to remove a very thick brown scale throughout the metal surfaces. After preservation and cleaning of the sample, the NDT such MPI was conducted to detect any of surface or subsurface defects (i.e. cracks) on the sample. Then, it was sectioned to reveal the internal surfaces which were found to be covered with a several small pits at the tubing wall. The sectioning processes were provided both fractography (e.g. pitting) and metallography (e.g good part) specimens. The metallography specimens were mounted using a hot mounting where heat and pressure was applied. While the fractography samples were mounted using a cold mounting so that it can be easy to cutting through the mounted sample (since it is transparent mounting) for investigate the localized pitting and scale. Then, the metallography samples were ground using various available grades (120, 240, 320, 400, 600, 800 & 1200 grit) to minimize thickness of damaged layer from the sectioning process. After grinding processes have been completed, these samples were polished (6, 1 μm) using a semi automated equipment to produce a scratch free mirror finish on the samples. A polished samples were etched by immersing the samples with the etchant (e.g. 2% Nital for steel) to remove the final thin layer of deformation. After that, the macroscopic examinations were conducted for both metallography and fractography by using OM with lower magnification (ranging from 50-1000x). Next, the microscopic examinations were performed for both metallography and fractography by using SEM with higher magnification (usually greater than 1000x) provided with the chemical analysis (e.g. EDS). Then, the analysis of metallographic sections was done in order to identify the microstructure of the material. Also, the determination of failure mechanism was determined the cause of failure due to some evidence that has been founded from SEM and EDS analysis. Finally, the predictions of failure mode were done provided with suggested solution. The following are the typical steps involve in failure analysis investigations [3]:

- *Collection of background data & selection of samples:* all the pertinent details including the manufacturing, service history and sequence of events leading to failure are being collected. Also the sample of the failed component (fractography) as well as good part (metallography) will be selected.
- *Preliminary examination of the failed part:* the preliminary examination of part will be performed to determine preliminary failure mode. Also the part will be photographed with special attention paid to anomalies (fractures, scratch, unusual mark, etc.).
- *Nondestructive testing (NDT):* to detect any defects related to the failure (cracks, porosity, slag inclusion, etc.) by using a common inspection techniques such as magnetic particle inspection (MPI), die penetrant test (DPT), ultrasonic testing (UT), radiography testing (RT) or eddy current.
- *Mechanical testing:* to determine on how the microstructure of a material could affect its properties by using a special testing such as hardness test, tensile test or charpy impact test.
- *Selection, identification, preservation and cleaning of all specimens:* to avoid mechanical or chemical damage. The sample was cleaned by using detergents, solvents or acetate replication to preserve residue on fracture or other surface of interest.
- *Samples Preparation:* there were some processes involved such as sectioning, mounting, grinding, polishing and etching for optical and scanning electron microsrocope (SEM). The following are details of the above explanation:-

Figure 3.1: Abrasive Cutter Machine

1) Initially the received sample was sectioned to obtain both metallographic and fractographic specimens. In failure cases, specimens were taken from regions immediately adjacent to failure surface. Cutting by using abrasive cutter may produce deformation damage as much as 1mm, could be minimized by using thin cutting disks.
2) Next, the cut samples were mounted either by cold or hot mounting press for ease of handling of difficult shapes and sizes, edge protection and also allow for easy labelling and identification of samples.

Figure 3.2: Grinder Machine

3) The mounted samples were then ground in order to minimize the thickness of damage layer from the sectioning process. The grinding process typically done using rotating discs covered with SiC paper and using water as lubricant. The various available grades are 120, 240, 320, 400, 600, 800 and 1200 grit (grains per square inch). Initial abrasive size establish a flat sample surface and remove damaged layer due to sectioning but subsequent abrasive sizes remove damaged due to previous grinding steps.

Figure 3.3: Polisher Machine

4) Polishing was conducted after at least 400 grit grind to produce a scratch free mirror finish on the sample. The polisher consists of rotating discs covered with soft cloth impregnated with micro-particles of diamond or other lubricant. The typical rough polishing of 9, 6, 3 µm diamond meanwhile final polishing of 1, 0.25 µm diamond.
5) Etching is a final step involved in preparing the sample before reveal the microstructural features under optical and scanning electron microscope. The purpose of etching is to remove the final thin layer of deformation. Usually, the polished sample is etched by immersing the sample with the etchant. Etching should be done in stages, beginning with light attack, an examination in the microscope and further etching if only required. An over-etched sample requires a repeat of polishing procedure.

- *Macroscopic examinations:* low magnification micrograph (magnifications ranging from 1-100x) for both metallography and fractography by using optical microscope (OM).

Figure 3.4: Optical Microscope

- *Microscopic examinations:* high magnification micrograph (magnifications usually greater than 100x) for both metallography and fractography by using scanning electron microscope (SEM). The nature of fracture can be obtained from microscopic examination of the fracture surface. Also, SEM provides the elemental analysis using Energy Dispersive Spectroscopy (EDS/EDX).

Figure 3.5: Scanning Electron Microscope

- *Analysis of metallographic sections:* to determine the microstructural features of the material.
- *Chemical analysis:* additional tool for microstructural analysis and characterization methods (e.g. X-Ray Fluorescence/XRF).

- *Determination of failure mechanism:* to determine the cause of failure.
- *Analysis of all evidence and formulation of conclusion:* to suggest the mode of failure provided with solution.

3.2 Gantt Chart

The Overall Project Milestones for 2-Semester Final Year Project were shown in Appendix V and VI.

3.3 Tool/Equipment Required

- Carbon Steel Tubing Cut Sample
- Failure Analysis Laboratory Equipments

CHAPTER 4

RESULTS AND DISCUSSION

4.1 Visual Examinations

The visual examinations indicate that the comparison of the observations for new steel tubular obtained from manufacturer before (refer to Figure 4.1) and after the extent during the service (refer to Figure 4.2).

4.1.1 Steel Tubular Product (before operation)

Figure 4.1: The grade L80 pipe of new steel tubular.

The Figure 4.1 shows the 2 ft length of new steel tubular product made by seamless process with 88.9 mm of outer diameter (OD) and 76.0 mm of inner diameter (ID) that was supplied by Halliburton Company for the use of typical water injection well. This steel tube with the grade of L80 pipe normally has been specified with the wall thickness of 12.7 mm [14].

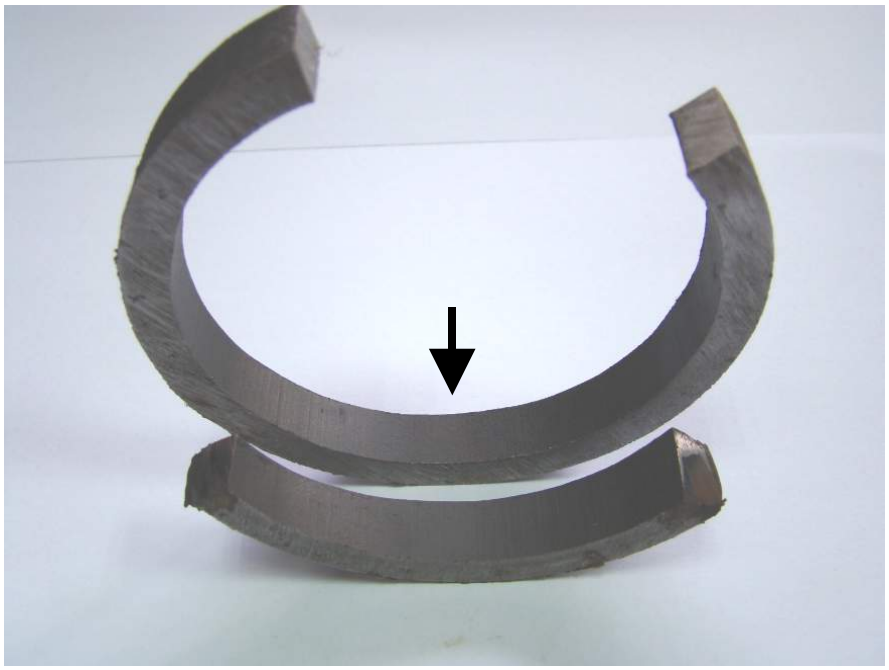

Figure 4.2: Photograph showing the internal surfaces of seamless tube.

Figure 4.3: Close-up photograph on internal surfaces of seamless tube.

Photographs of internal surfaces of the seamless tube were taken (see Figure 4.2). The arrow in Figure 4.2 shows the approximate location of Figure 4.3. The close-up examination on internal surfaces of tube as indicated in Figure 4.3 shows that there

was no indication of seam/defects that has been introduced during the manufacturing process.

4.1.2 Steel Tubular Product (after operation)

Figures 4.4, 4.5 and 4.6 show the photographs of the failed steel tube after the extent during the service with seawater. The failed product was traced on forming of pinhole that penetrates through the tubing wall and the formation of several small pits that has been introduced throughout the internal and external surface of the steel tube.

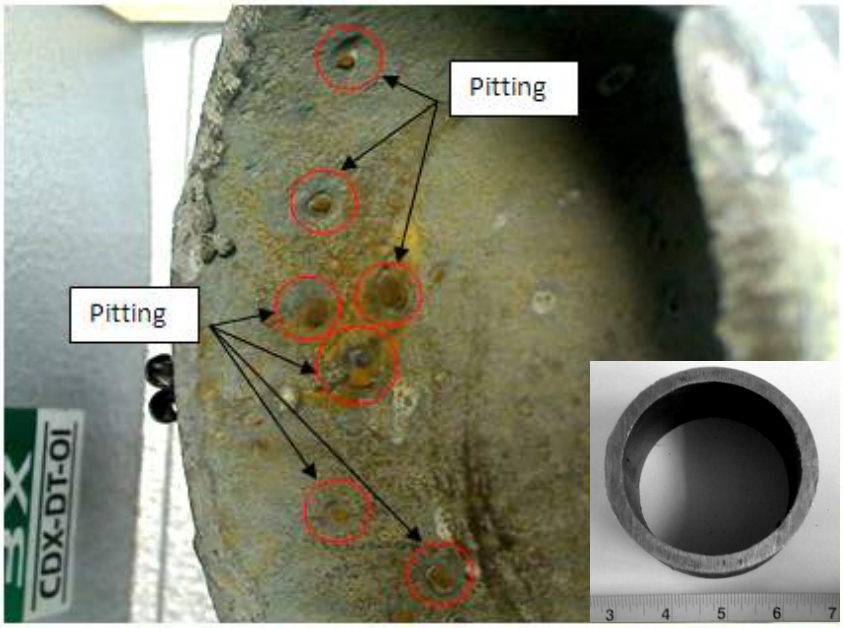

Figure 4.4: The internal surface of tubing cut sample.

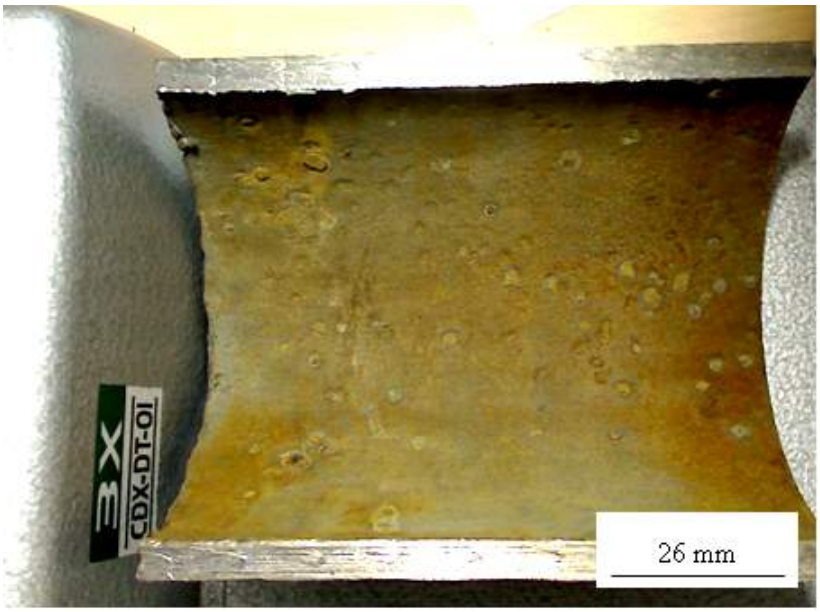

Figure 4.5: The internal surface of tubing cut sample showing extensive pitting.

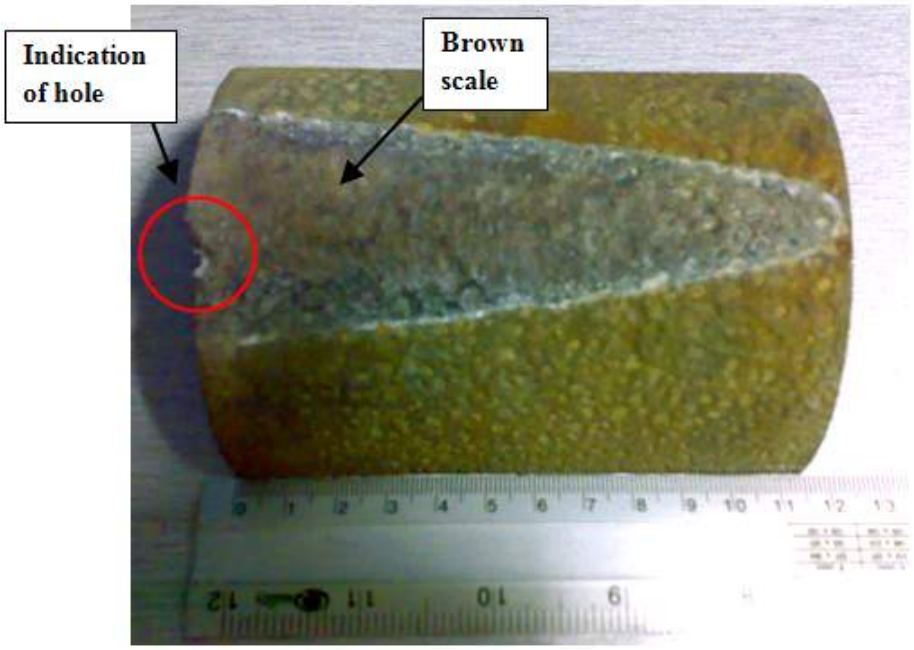

Figure 4.6: The external surface of tubing cut sample showing extensive pitting.

The investigations began when steel tubing cut sample was received for analysis. This was immersed into a chemical solution for a day in order to remove a very thick brown scale throughout the metal surfaces (refer to Figure 4.4). Beneath this

brown layer, pit penetrating into the tubing wall was resulted in hole (see red marked in Figure 4.6). Furthermore, localized deposits of corrosion product in the form of pitting were also evident (see arrow in Figure 4.4). Some tubular was sectioned to reveal the internal surfaces which were found to be covered with a several small pits at the tubing wall (refer to Figure 4.5). A deposit build-up of corrosion product on the both surfaces in same location was also observed. There was some evidence of attack on others areas of the tube.

4.2 Nondestructive Testing (NDT)

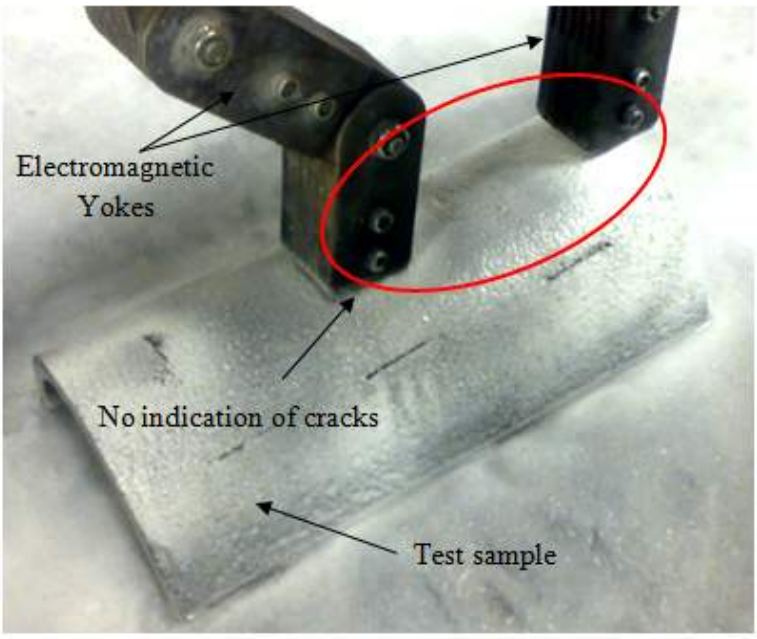

Figure 4.7: The magnetic particle inspection on tubing cut sample.

After preservation and cleaning of the sample, the nondestructive testing (NDT) such magnetic particle inspection (MPI) was conducted to detect any surface or subsurface

defects (i.e. cracks) on the tubular sample as shown in Figure 4.7. As a result, there was no evidence of any defects presence on internal and external surfaces of the failed steel tubular (refer Figure 4.7). If discontinuity is founded at any surface of tubular sample, the leakage of magnetic field will indicate the defect.

4.3 Mechanical Testing

According to American Petroleum Institute standard for casing and tubing (API 5CT), the hardness was specified as HRC 21 to 23 for grade L80 pipe although the material specification did not give any details on the specific measurement required to obtain this range [14]. From the measurements, the hardness Rockwell 'C' of the tube after the operation ranged between HRC 20 – 22 is shown in Table 4.1. This hardness value is normal for this particular type of steel and heat treatment condition. In the sections far from the perforation area, no variation either in the microstructure or in the hardness value between the outer diameter and the middle of the tubing wall. In contrast, the microstructure obtained close to the fracture surface was different but there was no variation in the hardness value between the middle wall and the outer diameter of the tube.

Table 4.1: Rockwell 'C' hardness measurement (HRC) of tube after operation.

Hardness measurement	Average (HRC)
Close to outer diameter	21.3
Middle wall	21.1
Close to internal diameter	20.7

4.4 Metallography

Macroscopic and microscopic examinations were conducted to observe both inclusions and the microstructural features. Also, they were performed to identify any abnormality in the microstructure that might have existed within the steel tubular and compare the

microstructure before and after the extent during the service. Typical features are shown in Figure 4.8, 4.9, 4.10 (a and b), 4.11, and 4.12.

4.4.1 Macroscopic and Microscopic Examinations (before operation).

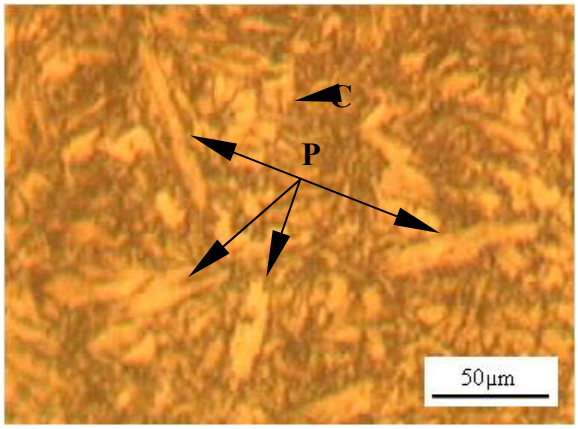

Figure 4.8: The optical micrograph of Fe-0.4C. 2% Nital etchant. Mag. 200x.

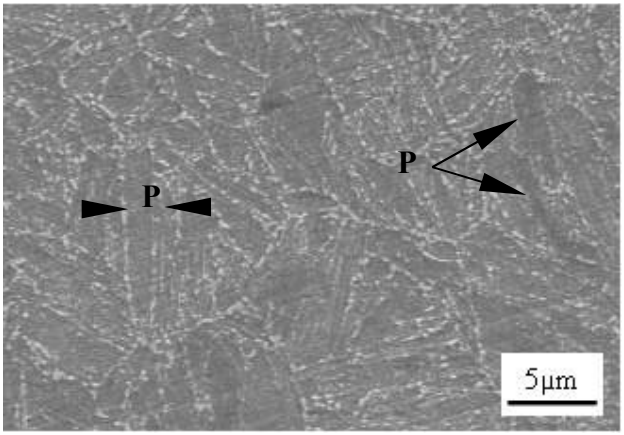

Figure 4.9: The scanning electron micrograph of Fe-0.4C. 2% Nital etchant. Mag. 2000x.

Transverse and longitudinal sections were taken respectively. These sections were metallographically prepared. The typical microstructure of the steel tubular was tempered martensite (see Figure 4.8) [9, 15]. The microstructure consists of ferrite and a few patches of tempered martensite. The present of plate martensites among the lath martensites are indicated by the region marked P (see Figure 4.8 and 4.9). The arrows marked C as in Figure 4.8 shows the formation of carbides precipitate, probably cementite particles with nital etched. The present of fine cementite was obtained due to high tempering temperature attained which was above 350°C during the heat treatment process. The detailed examination of the microstructure by scanning electron microscopy (SEM) confirmed that the microstructural feature developed for the steel tube was tempered martensite (see Figure 4.9).

4.4.2 Macroscopic & Microscopic Examinations (after operation).

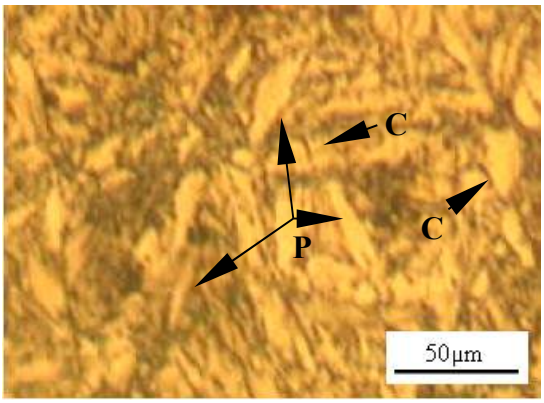

Figure 4.10 (a): The optical micrograph of Fe-0.4C. 2% Nital etchant. Mag. 200x.

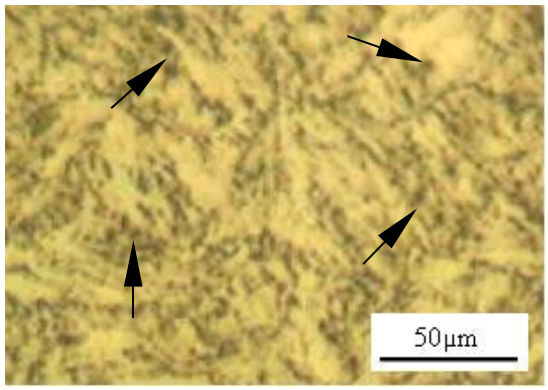

Figure 4.10 (b): The optical micrograph of Fe-0.4C. 2% Nital etchant. Mag. 200x.

Two metallographic cross sections were prepared from two different locations on the steel tube. Both of them were subjected to the extreme operating conditions during the service life. The two areas of the tube were examined and compared. The characteristic structures developed were tempered martensites (see Figure 4.10 (a) and 4.10 (b)) [9, 15]. The formation of two forms of martensite in the medium-carbon (0.4%) steel was clearly shown as indicated in Figure 4.10 (a). The presence of plate martensite among lath martensite were formed as individual in regions marked P as shown in Figure 4.10 (a). Also, the formation of fine carbides known as cementite (Fe_3C) were detected in the regions marked C as in Figure 4.10 (a) with nital etched. Meanwhile, the cementite particles became increasingly spheroidal in shape towards near the through wall hole as indicated by arrows in Figure 4.10 (b). Hence, there was an evidence of excessive thermal exposure near the through wall holes area during the operation. Moreover, most cementite particles were founded to be located at the ferrite grains boundaries (see Figure 4.10 (b)). The light phases appear as illustrated in Figure 4.10 (b) were ferrite probably due to the recovery and recrystallization of martensite (compare Figure 4.10 (a) and 4.10 (b)) due to continuous exposure on heating during the operation. At this stage, the ferrite grains continue to grow and gradually assume an equiaxed in shape. Although, the discrete grains of ferrite cannot be recognized clearly because of the confusion caused by the presence of many partly resolved of particles cementite and probably can be recognized after etching by appropriate techniques.

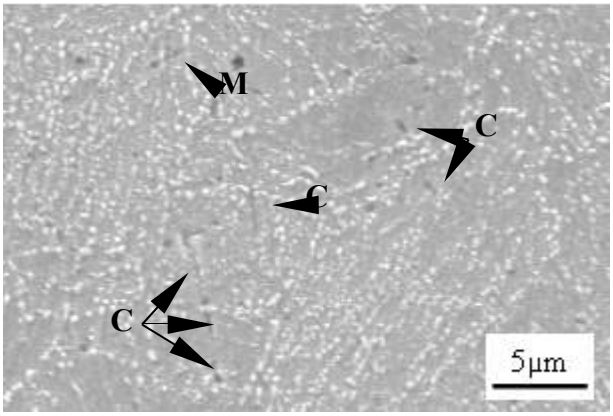

Figure 4.11: The scanning electron micrograph of Fe-0.4C. The arrows C show the fine cementite particles appeared as far away from the hole area. Mag. 2000x.

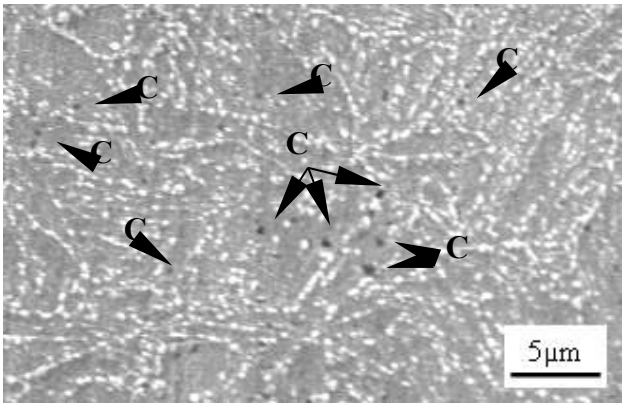

Figure 4.12: The scanning electron micrograph of Fe-0.4C. The arrows show the spheroidized cementite have been introduced towards near the hole area. Mag. 2000x.

Detailed examination of the microstructure by scanning electron microscopy (SEM) shows the same features of tempered martensites found in the steel tube (see Figure 4.9 and 4.10). The region marked C as in Figure 4.11 and 4.12 indicated that the presence of carbides precipitate probably cementite at two different locations. In both areas, the microstructures features were dissimilar and not uniform throughout. The SEM shows that the fine cementite particles appear as far away from the hole area (see Figure 4.11). Besides, the abnormality confirmed by SEM as indicated by the region marked C as in Figure 4.12 which show that the spheroidized cementites appear towards the through wall hole. This was probably due to the excessive thermal exposure near the through wall holes area during the operation. Also, an arrow M indicates as a probable microcrack, an intragranular microcrack which runs transversely in regions of plate martensite. That arrow identified as a probable microcack because the feature was aligned perpendicular to the direction of major arrays of cementite particles (regions marked C in Figure 4.11). This indication was probably due to cracking produced during quenching.

4.5 Fractography

Visual examination of the failed cross section of the tube at the through wall hole. The photographs present the fracture surfaces of the internal and external surfaces of the tube (see Figure 4.13 (a, b and c)). Later, the detailed examinations of these fracture surfaces were examined by using SEM.

Figure 4.13 (a): Photograph showing a cross-section of internal region of the tube through wall hole area (pointed by arrow).

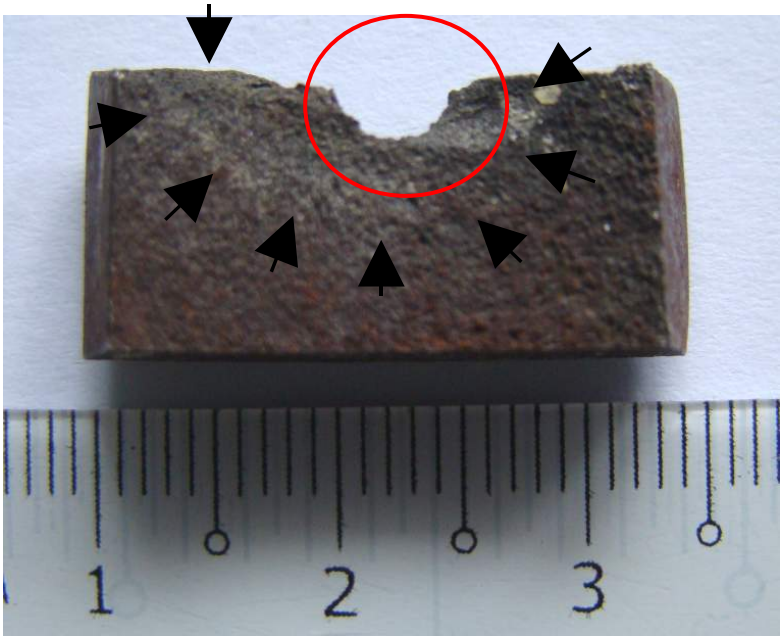

Figure 4.13 (b): Photograph showing a cross-section of internal surface of the tube at the hole area (region marked red).

Figure 4.13 (c): Photograph showing a cross-section of external surface of the tube at the hole area (pointed by arrow).

Figure 4.13 (a, b and c) show severely pitted region in cross-section. The visual examinations results indicate that the tube was attacked in localized area on both internal and external surface of the tube in the form of pitting. Also, the internal surface of the failed tube contained a region of severe metal loss (pointed by arrows) as indicated in Figure 4.13 (b). In addition, it was clearly shown that (refer Figure 4.13 (c)) the large and deep pit has been form on the external surface of tube. Thus, the attacked penetrated the tube wall and resulted in through wall hole.

4.5.1 Scanning Electron Microscopy

A section containing the hole area was removed for examination in a SEM equipped with an Energy Dispersive X-Ray Spectroscopy (EDX). SEM examination revealed the internal side of the tube was attacked by the numerous of pitting (see Figure 4.14 (a)). Figure 4.14 shows close-up photographs of the attack at the hole area where the corrosion pits were present and the EDX plot is shown in Figure 4.15. However, the

sample of the corrosion product was further examined using SEM (see Figure 4.16) and EDX plot showed a marked presence of iron oxide (see Figure 4.17).

(a)

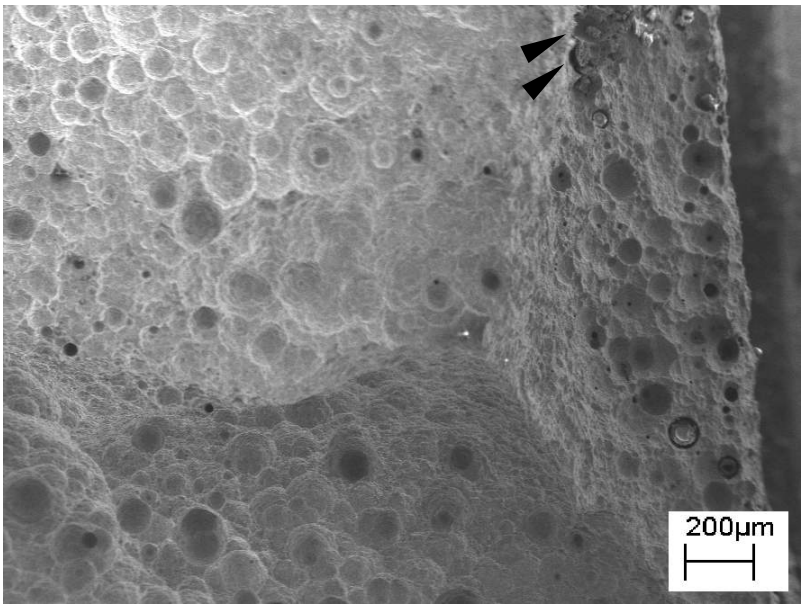

(b)

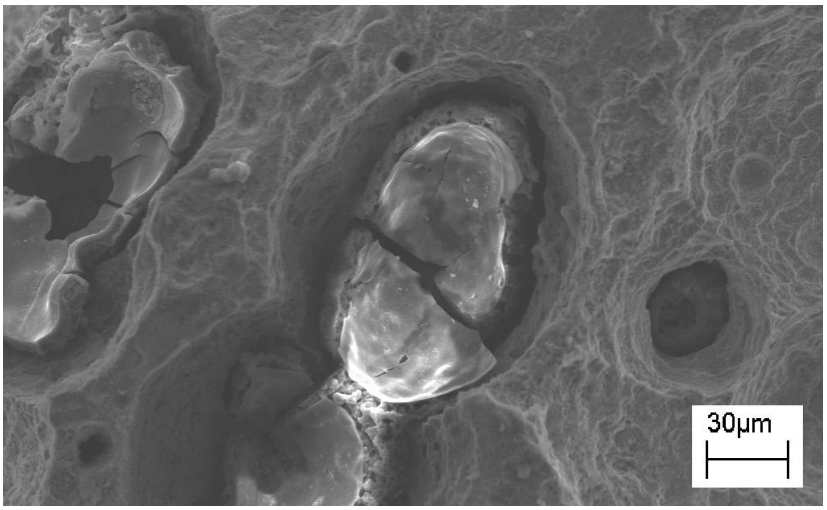

Figure 4.14: The scanning electron fractograph of Fe-0.4C. The arrows in photograph (a) show the approximate close-up location of photograph (b). (a) Mag. 50x. (b) Mag. 200x.

Energy Dispersive X-Ray Spectroscopy (EDX) indicated that the internal region of the tube through wall hole area consisted primarily of iron (56.5%) and manganese (19.4%) with minor trace amounts of carbon (6.3%) and copper (5.1%) as shown in the Table 4.2. This was noted that the elements appear above in the EDX analysis was those originated from the base metal.

Table 4.2: Chemical analysis (wt %) of the failed tube at the hole area.

Element	C	Fe	Mn	Cu	Cl
Weight (%)	6.3	56.5	19.4	5.1	12.7

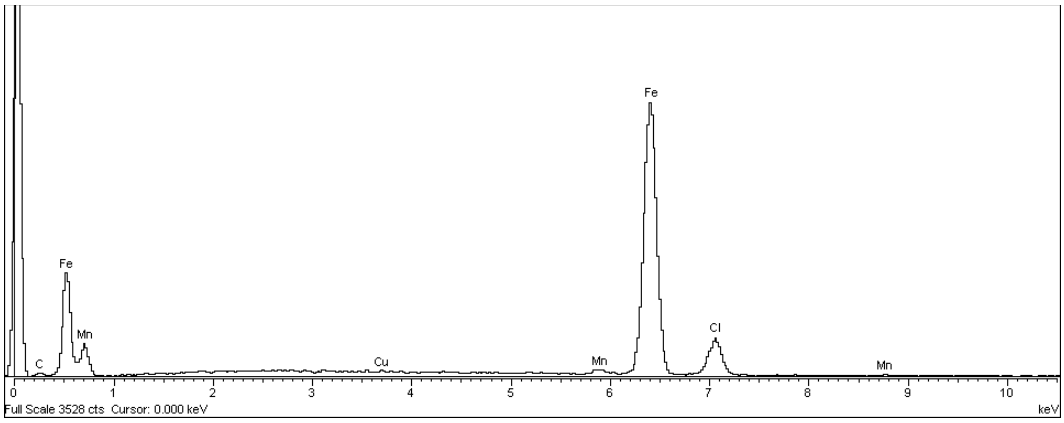

Figure 4.15: The EDX elemental analysis results of the internal side of the tube through wall hole area.

In addition, the results of the analysis revealed that the corrosion pits was high in chlorine (12.7%). The presence of the chlorine probable due to continuous exposure of the tube on the seawater during the extent of the service. Here it was hypothesised that metal surface of the tube was attacked by the chloride containing acidic environment from the seawater and lead to start of pitting. This corrosion rates increased with temperature as the tubing goes deeper into the target reservoir formation. Thus, the heated seawater may deposit protective scale or lost of its oxygen on the pits area and accelerate the corrosion attack. The results of deposits on the pits area tends to restrict the oxygen access and lead to crevice corrosion attack. Therefore, this localized attack will developed the severe form of pitting that results in through wall hole on the steel surface.

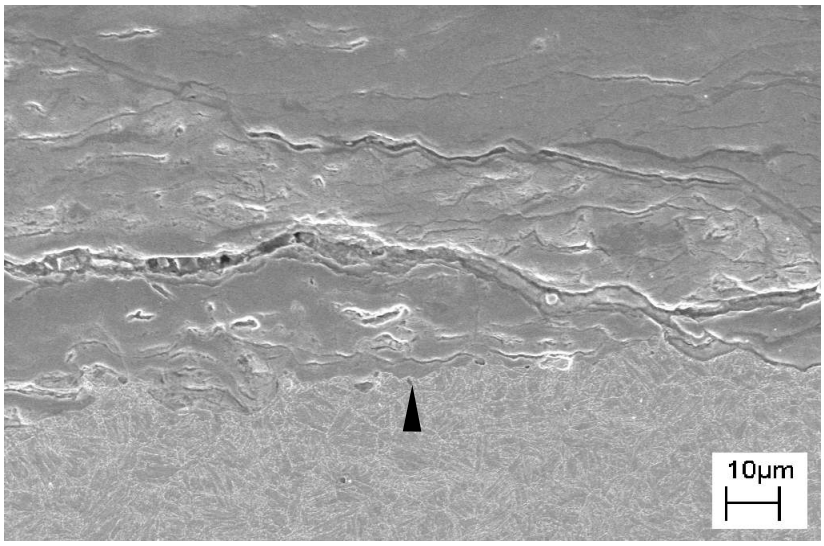

Figure 4.16: The corrosion product analysed using EDX. Mag. 500x.

Figure 4.16 shows the scanning electron micrograph of the tube internal surface and scale deposit in the region of metal loss. The arrow in this figure indicated that the interface between the deposited scale and steel surface on the pitted area.

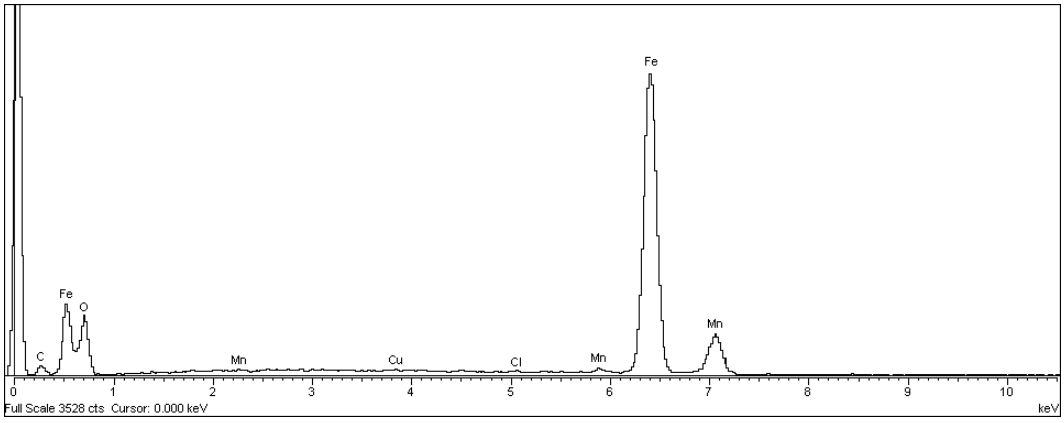

Figure 4.17: The EDX analysis of the corrosion product showed a marked presence of iron oxide and chlorine.

Figure 4.17 shows the EDX results of the corrosion residue present at the pitted region. The iron, manganese, carbon and copper peaks in Figure 4.17 arise from the carbon steel itself. The results of the analyses revealed that the steel tubular was being chemically corroded by chlorine compounds from the seawater. At the

interface between the pit and adjacent surface, iron hydroxide will be formed due to the interaction between hydroxide ions from seawater and metal surface. This will further oxidised by the dissolved oxygen in seawater to form iron oxides and therefore detected in scale deposits. There was not enough of the corrosion residue present to conduct X-Ray Diffraction (XRD) analyses to determine the specific corrosive compounds and iron oxides compounds.

CHAPTER 5

CONCLUSION AND RECOMMENDATION

5.1 Conclusion

As mentioned above, the typical microstructure of the steel tubular with grade L80 pipe was tempered martensite in accordance with the thermal treatment of quenching and tempering suffered by this material. The change in microstructure of the tube towards near the hole area showed evidence of localized overheating due to continuous thermal exposure during the operation. It was concluded that the failure of the steel tubular was due to pitting and crevice corrosion attacked. It was clear that the exact cause of pitting failure was particularly due to the extent of service during the operation. It was highly suggested that the failure probably due to the chloride attack originated from the seawater during the extent of the service. Here it was hypothesised that the severe form of pitting resulted due to the crevice corrosion attack in the present of the scale deposited at the pits area.

5.2 Recommendation

It is therefore recommended that the steel tubular should be replaced by using AISI type 316 Stainless Steel that susceptible to pitting and crevice corrosion attack. From the literature, it was noted that the AISI type 316 Stainless Steel exhibit excellent corrosion resistant to pitting and crevice corrosion [16]. In addition, this 300 series type of steel exhibit some degree of susceptibility to Stress Corrosion Cracking (SCC). The present of chromium is the element essential in forming the passive film in 316 Stainless Steel. Meanwhile, molybdenum in combination with chromium is very effective in terms of

stabilizing the passive film in the present of chlorides. Molybdenum is especially effective in increasing resistance to the initiation of pitting and crevice corrosion.

REFERENCES

1. Roemex Ltd. 2005 <http://www.roemex.com/production/water_injection.htm>.

2. TTC 1995, *Wireline Operations Training Manual*, Western Australia, R.J.Taylor

3. Marcel Dekker, Inc. 2004, *Practical Engineering Failure Analysis*, Unites States of America, Hani M. Tawany, Anwar Ul-Hamid & Nureddin M. Abbas

4. Taylor & Francis Group 2007, *Steel Heat Treatment*, Unites States of America, George E. Totten

5. McGraw-Hill, Inc. 1987, *Corrosion Engineering*, Singapore, Mars G. Fontana

6. Shahrizal Hashim. 10 August 2008 <https://workforce.petronas.com.my>.

7. Shahrizal B. Hashim, Well Services Engineer. PCSB, Kertih. Personal Interview. August 10. 2008

8. Sunny Steel Enterprise Ltd. 2008 <http://www.sunnysteel.com>.

9. American Society for Metals, 1999, *Light Microscopy of Carbon Steels*, Unites States of America, L.E. Samuels

10. NACE International, 1982, *Forms of Corrosion: Recognition and Prevention*, Houston, Dillon CP

11. McGraw-Hill, Inc. 2008, *Corrosion Engineering: Principles and Practice*, United States of America, Pierre R. Roberge

12. McGraw-Hill, 2000, *Handbook of Corrosion Engineering*, New York, Roberge PR

13. DECHEMA e.V., 2005, *Corrosion Handbook,* **(5),** Germany, Gerhard Kreysa & Michael Schutze

14. American Petroleum Institute, 1999, *API Spec 5CT*

15. ASM International, 1987, *ASM Handbook,* **(9),** United States of America, Taylor Lyman

16. ASM International, 1987, *ASM Handbook,* **(13),** United States of America, Taylor Lyman

APPENDICES

Appendix I: The Existing Completion Diagram on Well DLA-29

Appendix II: The Existing Completion Diagram on Well DLA-32

Appendix III: The Existing Completion Diagram on Well DLC-25

Appendix IV: Glosary of Terms

Appendix V: Project Milestone for the First Semester of 2-Semester Final Year Project

Appendix VI: Project Milestone for the Second Semester of 2-Semester Final Year Project